Characterization of pore geometry of reservoir rocks in relation to their interactions with supercritical CO_2

Teng-fong Wong, *Department of Geosciences*
State University of New York, Stony Brook, NY 11794-2100

Geologic Storage of CO_2: Injectivity and Integrity

- **The injection and movement of CO_2 perturb the pore pressure and effective stress, which would impact the integrity of both cap rock and reservoir rock.**
- **Significant thermodynamic disequilibrium between the pore fluids and host rock may develop, thus promoting geochemical reactions which may alter the mineral assemblage and porosity, and in turn lead to irreversible changes in permeability, mechanical strength and other physical properties.**

Geologic Storage of CO_2: Injectivity and Integrity

- Reactive flow can potentially alter the mineral assemblage and porosity, and in turn lead to irreversible changes in physical properties.
  - Dissolution of carbonates (present either as a rock forming mineral or as cement) may enhance the porosity and permeability, leading to mechanical weakening and enhanced compaction.
  - In contrast, precipitation may occur if the fluids were to become supersaturated with carbonate minerals as the CO2 plume migrates to relatively long distances from the injection well. This would decrease the porosity and permeability, and possibly strengthening the reservoir rock.
- Most data on the kinetics of dissolution and precipitation are for carbonate minerals and crushed rocks. In comparison, there is a paucity of data on lithified rock.

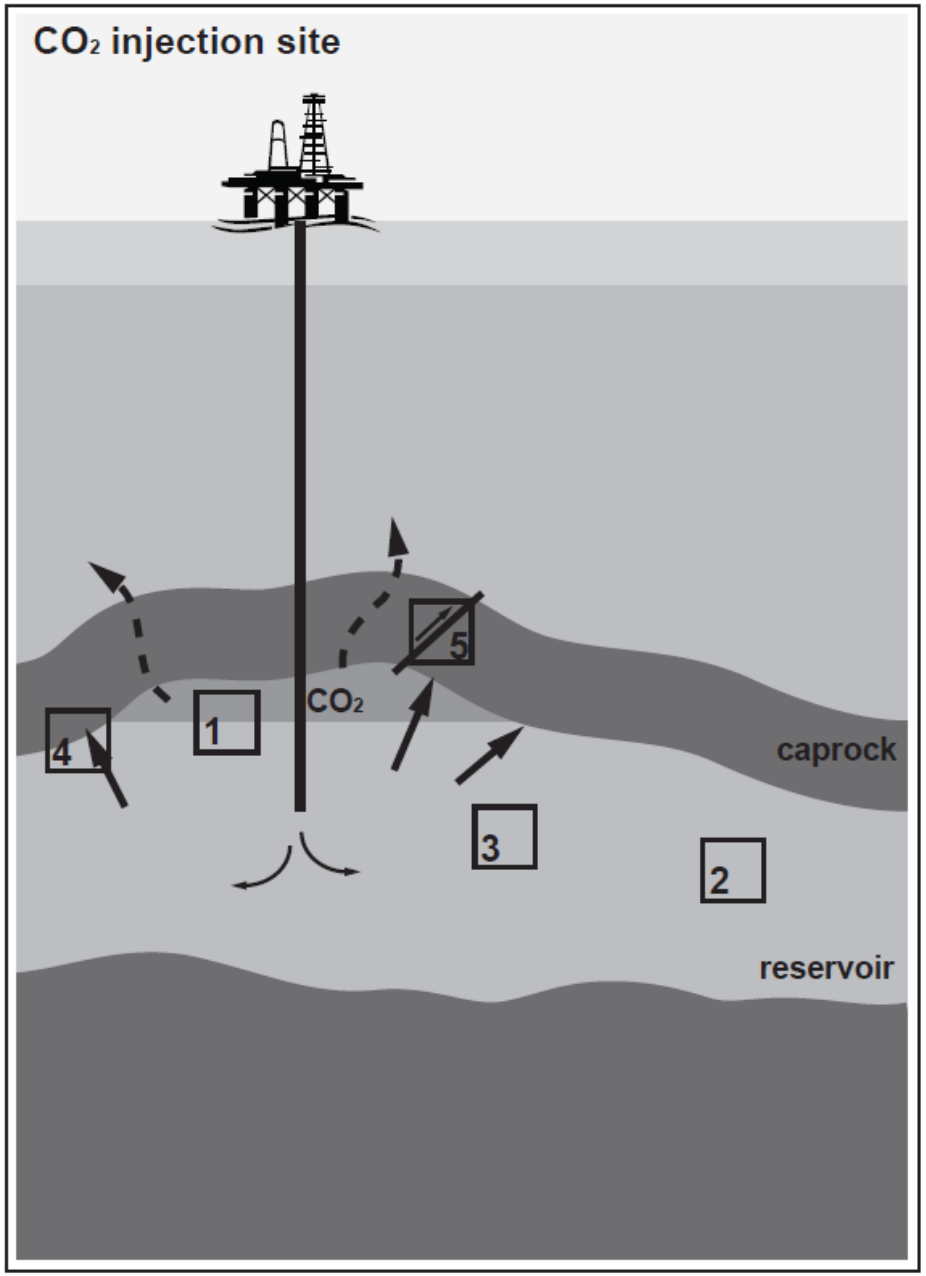

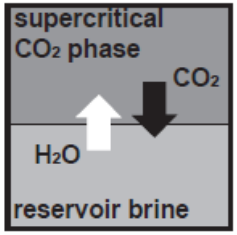

1. Solubility trapping occurs as the injected CO_2 moves through the reservoir and slowly dissolves into the reservoir brine, leading to an acidification of the pore fluid. In addition, water may dissolve into the CO_2, which may result in dessication of the reservoir.

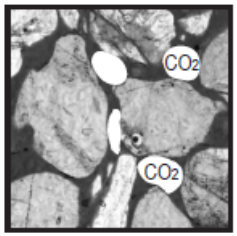

2. Residual trapping is the trapping of CO_2 in the pore space as a result of the high interfacial tension and capillary pressure of the CO_2 phase.

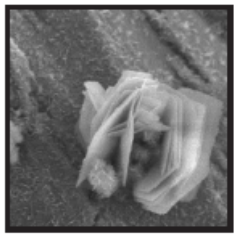

3. Mineral trapping occurs due to chemical interaction between the (acid) reservoir fluid and (alumino)silicates may result in the fixation of CO_2 in the form of stable carbonate minerals.

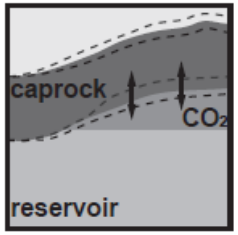

4. Structural trapping: compaction/expansion of the reservoir and bending of the caprock may result in reactivation of pre-existing faults in the reservoir, overlying caprock or overburden.

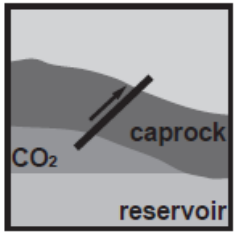

5. Structural trapping: induced shear fracturing can occur in the host and seal formation as a result of reservoir compaction or expansion, and leads to the formation of new faults, which may serve as preferential CO_2 leakage pathways.

Hangx (2009)

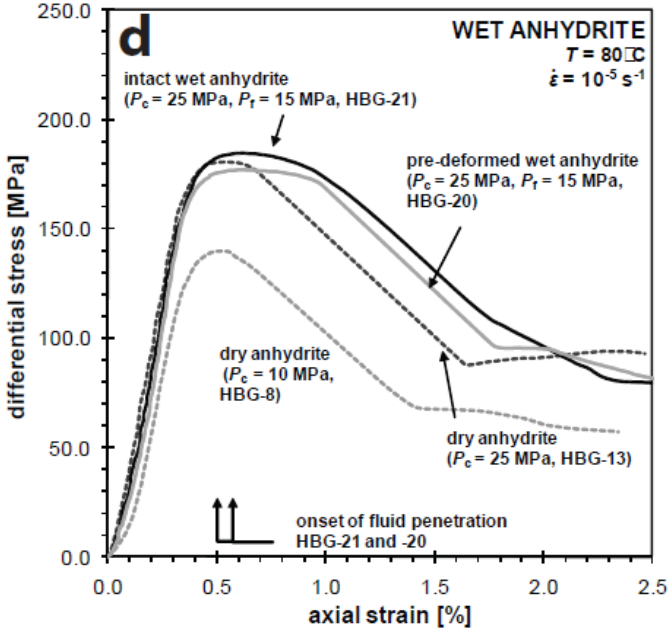

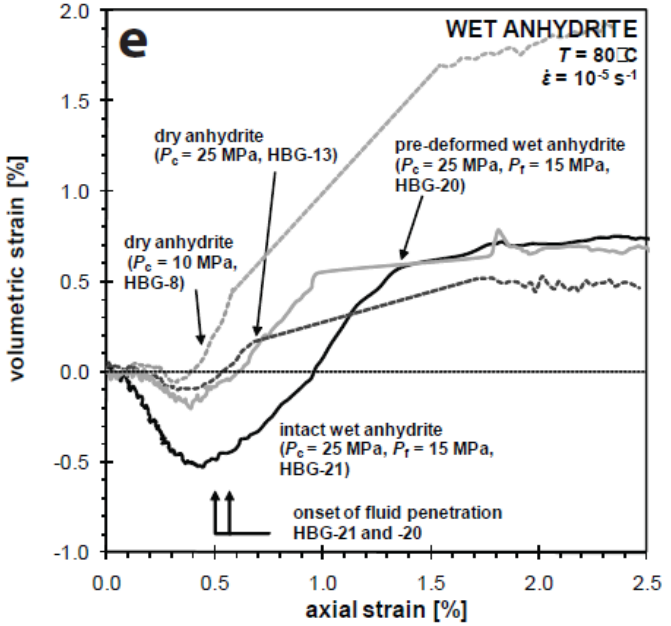

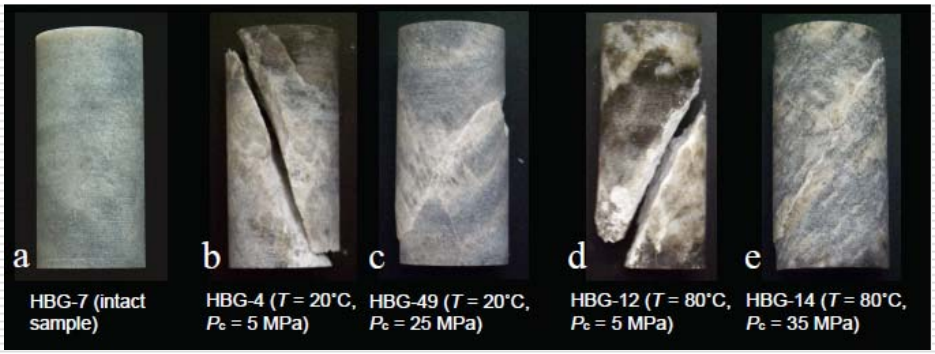

- Anhydrite provides the seal for many hydrocarbon reservoirs. It is also the caprock at several pilot CO_2 injections sites, including Teapot dome (Wyoming), Weyburn Field (Saskatchewan) and the K12-B Field (Holland).
- Mechanical data on brittle strength of anhydrite saturated with CO_2 and subjected to a static pore pressure show that the short-term chemical effect on strength is relatively small.

Hangx, Spiers & Peach (2010)

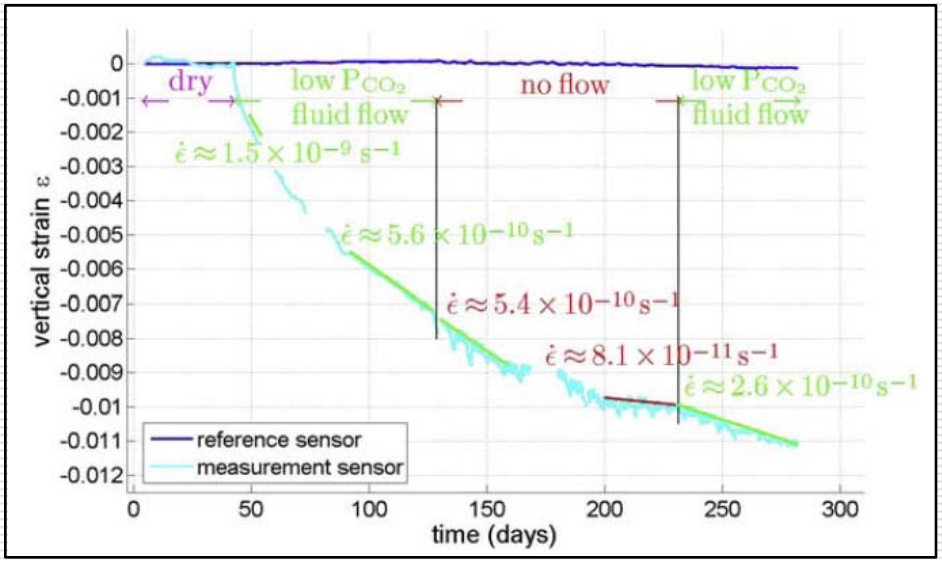

Lavoux limestone (23%)

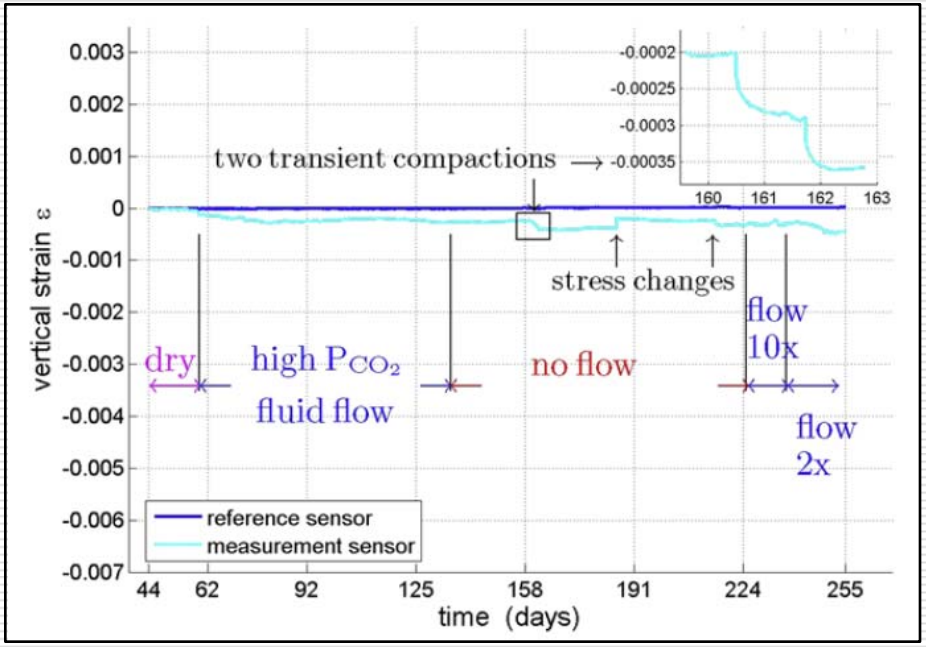

Triassic arkosic sandstone (16%)

- Enhanced creep was due to the acidification of the injected fluid, which induced significant increase in solubility and reaction kinetics of calcite. In comparison, quartz has lower solubility and reactivity.
- Deformation mechanisms – pressure solution, subcritical crack growth.

Rock sample	Lavoux W526	Sandstone
Fluid P_{co_2}	high P_{co_2}	high P_{co_2}
σ_1 (MPa)	16.3	16.0
σ_3 (MPa)	12.0	10.2
p_f (MPa)	7.9	8.3
σ_e (MPa)	8.4	7.7
P_{co_2} (MPa)	7.9	8.3
T (°C)	40	40
[NaCl] (mol l^{-1})	10^{-2}	10^{-2}
Fluid flow ($m^3\ s^{-1}$)	8.33×10^{-11}	8.33×10^{-11}
Residence time (h)	12.8	10.0
Fluid velocity ($m\ s^{-1}$)	1×10^{-6}	1.4×10^{-6}

Le Guen, Renard, Hellmann, Brosse, Collombet, Tisserand & Gratier (2007)

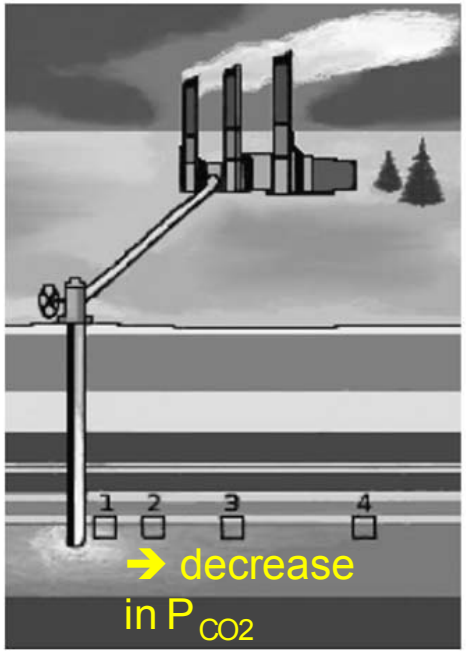

Fig. 1. Schematic illustration of a CO_2 storage facility in a sedimentary reservoir. Boxes 1 to 4 represent the decrease of CO_2 partial pressure along fluid transfer pathways into a host reservoir. For our experiments, in box 1: $P_{CO_2} = 10$ MPa (D1), box 2: $P_{CO_2} = 6$ MPa (D2), box 3: $P_{CO_2} = 2.5$ MPa (D3) and box 4: $P_{CO_2} = 0.7$ MPa (P1).

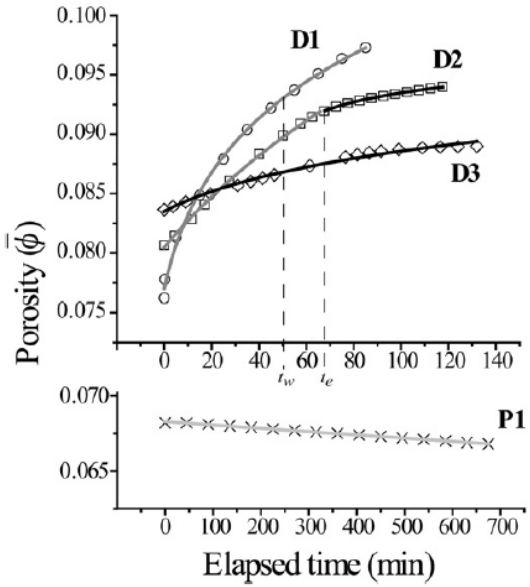

Fig. 10. Porosity calculated from Ca and Mg mass balance (Eq. (12)) for experiments D1 (circles), D2 (squares), D3 (diamonds) and P1 (crosses), and model curves (Eq. (14)).

Table 1
Water composition for experiments D1, D2, D3 and P1.

Species (mmol l^{-1})	D1	D2	D3	P1
Na	1000	1000	1000	1000
Ca	8.25	9.37	10.0	87.5
Mg	0.16	0.19	0.21	1.85
Cl	1000	1000	1000	1000
CO_2 (mol l^{-1})	0.8	0.5	0.2	0.06
P_{CO_2} (MPa)	10	6	2.5	0.75
pH	3.21	3.51	4.02	8.7
I_{out}	0.22	0.28	0.60	–
I_{in}	$1.9 \cdot 10^{-4}$	$5.3 \cdot 10^{-4}$	$22.4 \cdot 10^{-4}$	–

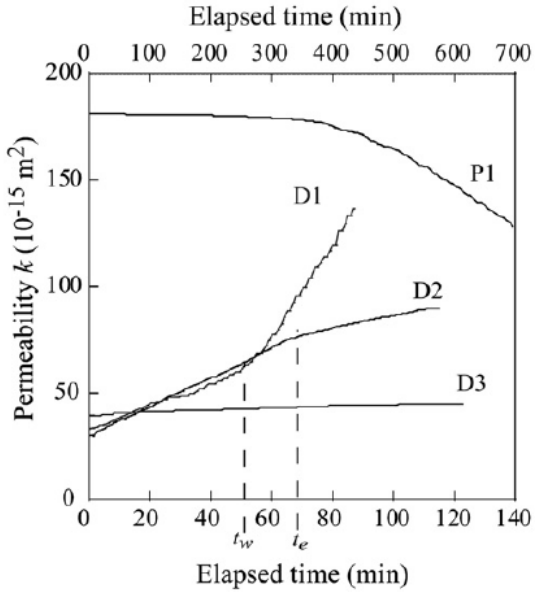

Fig. 11. Variation of sample permeability with elapsed time for the dissolution experiments (D1, D2 and D3) and the precipitation experiment P1.

Mondeville limestone, ~7% (*Loquot & Gouze*, 2009)

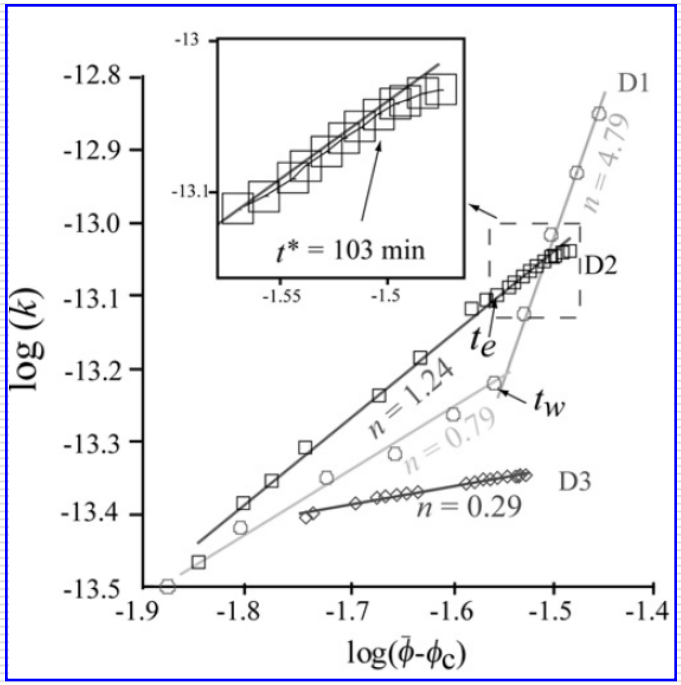

- There seems to be an overall trend for the Carman-Kozeny exponent to decrease as D1→D3.
- Interpretation is complicated by the observation that the samples (particularly D1 and D2) are associated with significant dissolution localization manifested by wormhole formation.

- Wormhole formation is inhibited by decrease in the Damköhler number associated with a transition from transport- to reaction-limited dissolution.
- The pore space has heterogeneities on two different scales.

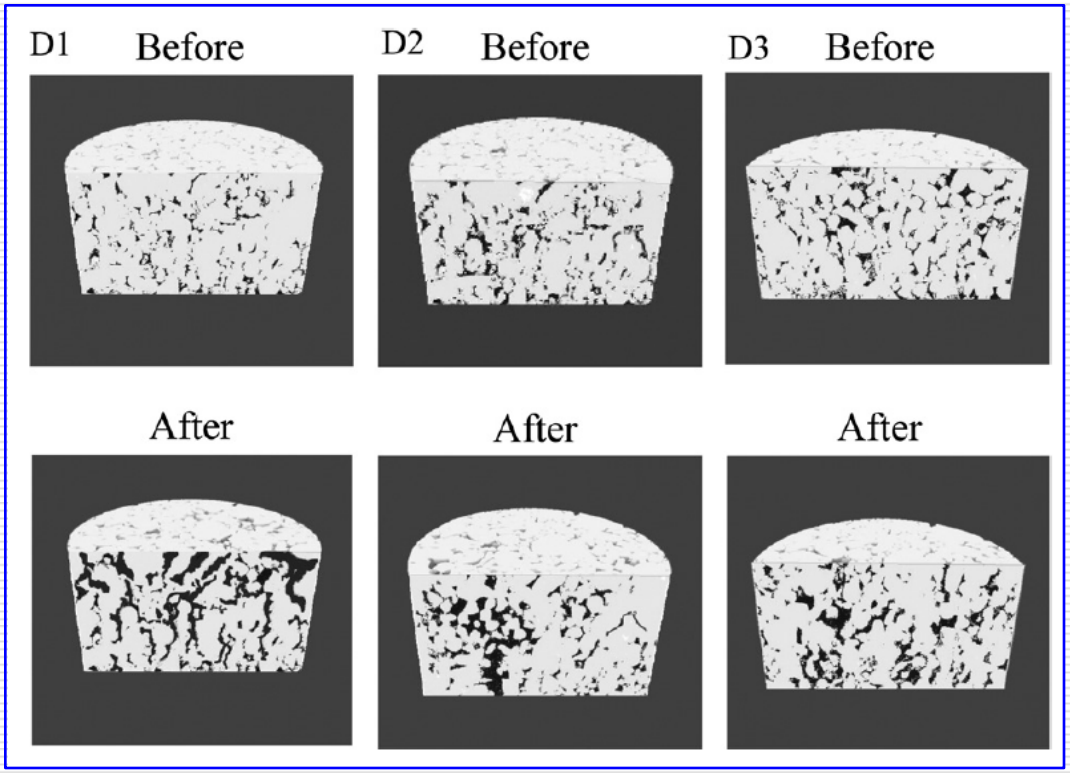

Upper Miocene limestone from Mallorca (~16%)

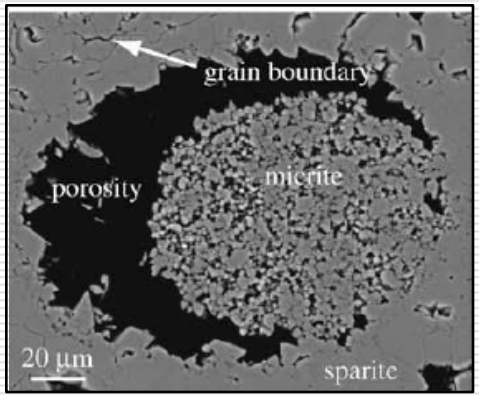

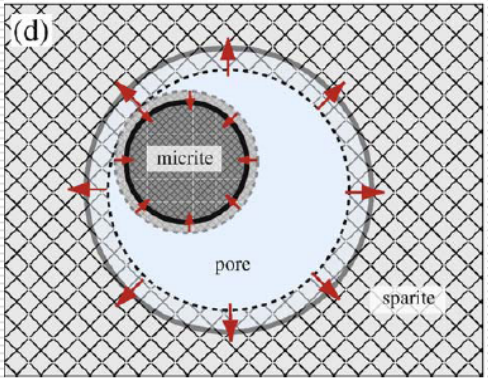

- Micrite grains and sparite crystals have different trace element signatures.
- The reactive surface area changes can be inferred from the Sr and Ca concentrations in the rock and the outlet solution.

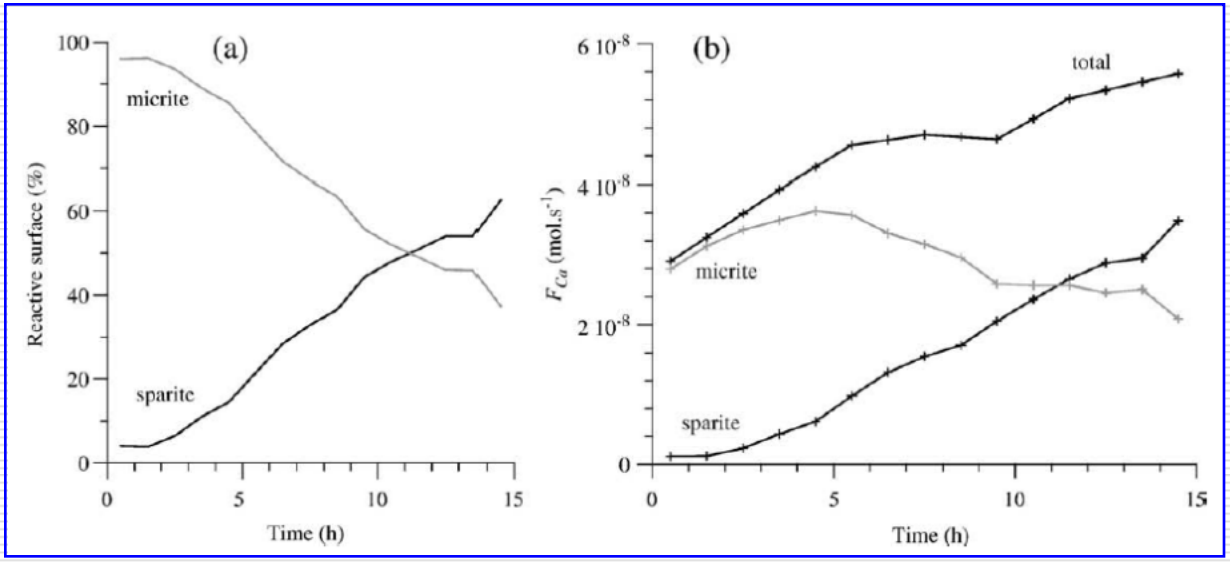

Noiriel, Luquot, Made, Raimbault, Gouze & van der Lee (2009)

- Preexisting microporosity in the micrites provide significant portion of the reactive surface area.
- Injection of CO_2-rich water increases the reactive surface area of the macropores and decreases that of the micropores.

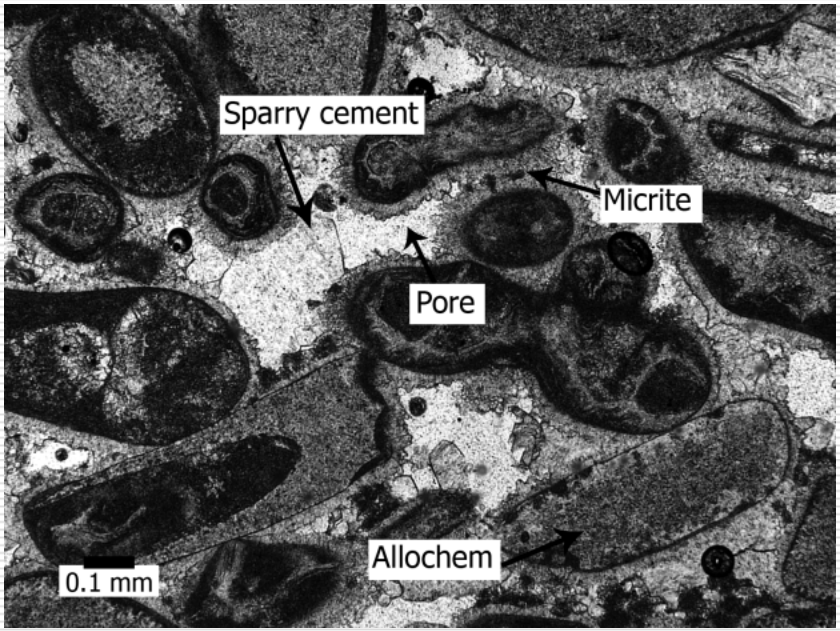

Vajdova, Baud, Wu & Wong (2011)

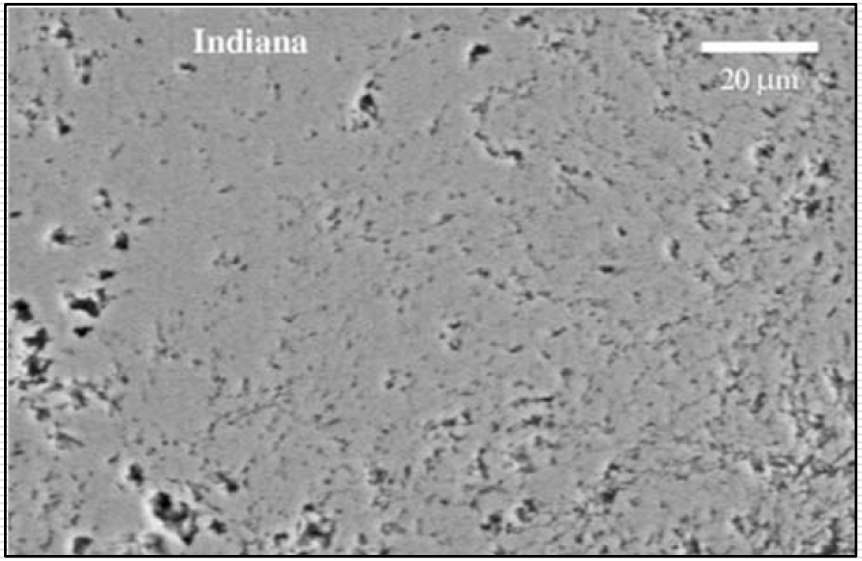

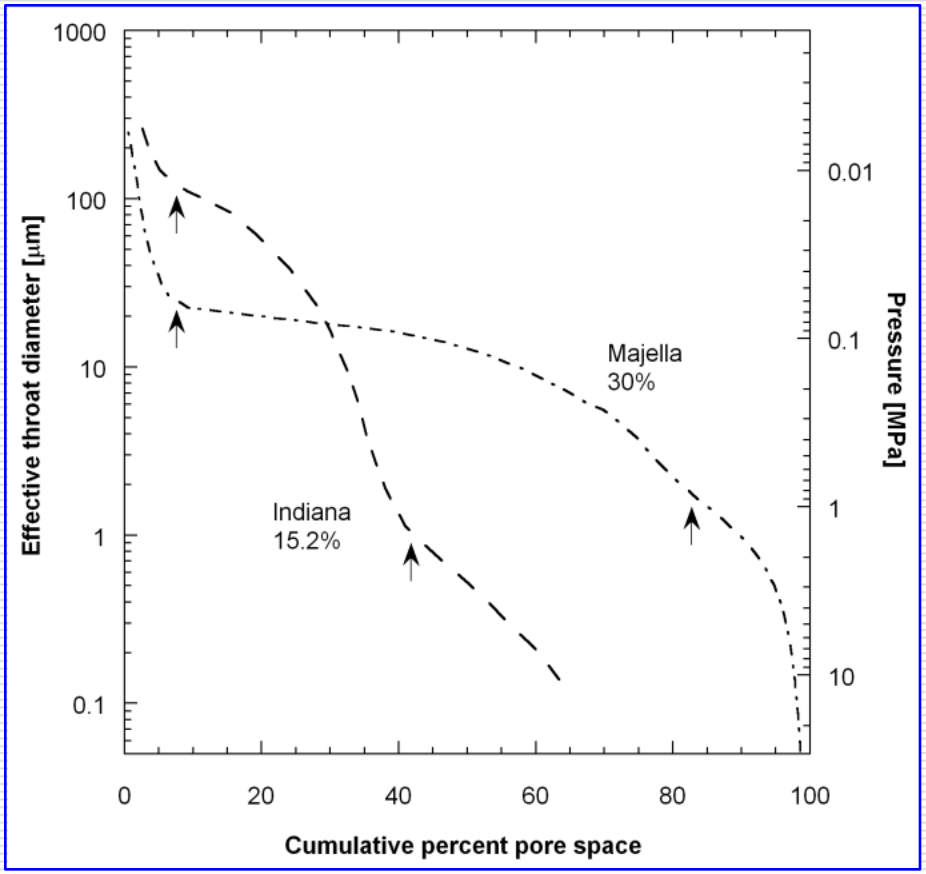

Mercury injection capillary pressure for Indiana (*Churcher et al.*, 1991) and Majella (*Baud et al.*, 2009) limestones

Macroporosity 4%

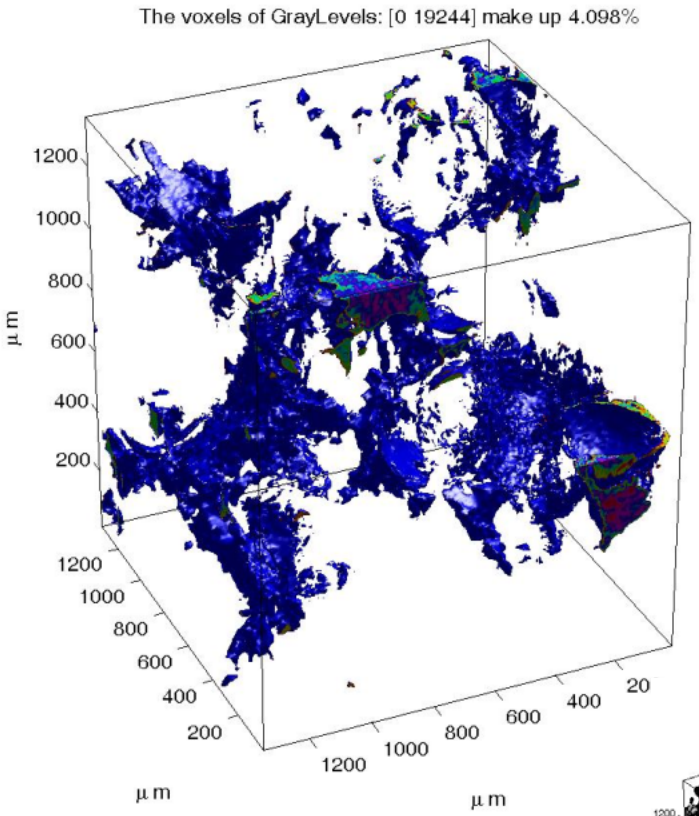

Solid 85%

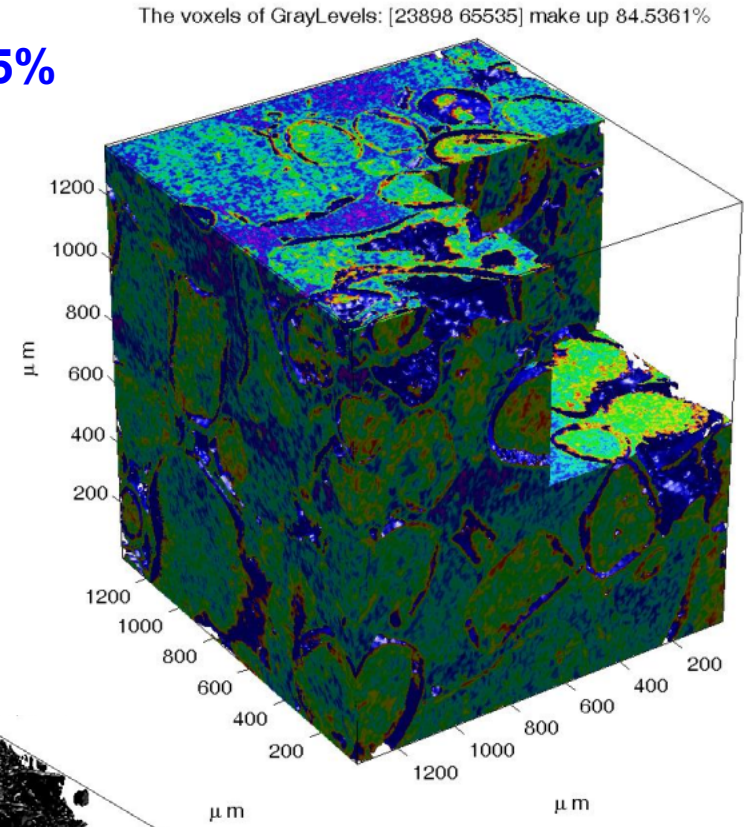

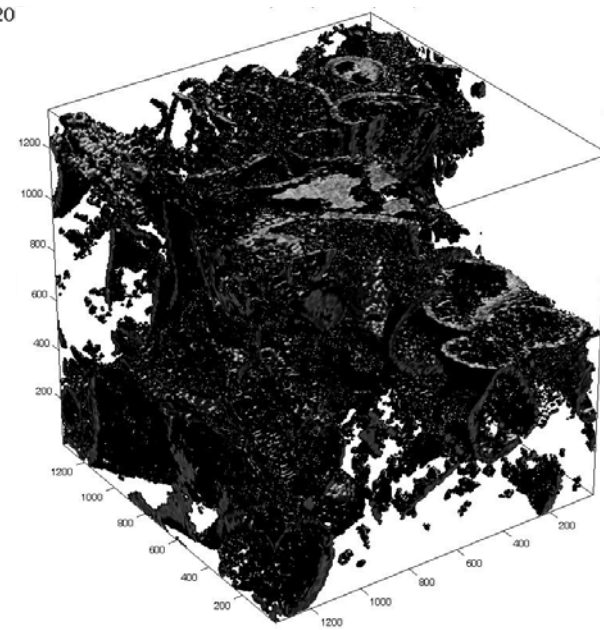

X-ray μCT image of Indiana limestone (4μm resolution) segmented into three domains (*Ji*, 2011)

Intermediate zone dominated by 11% microporosity ➔

X-ray μCT image of Indiana limestone (4μm resolution) segmented into three domains (*Ji*, 2011)

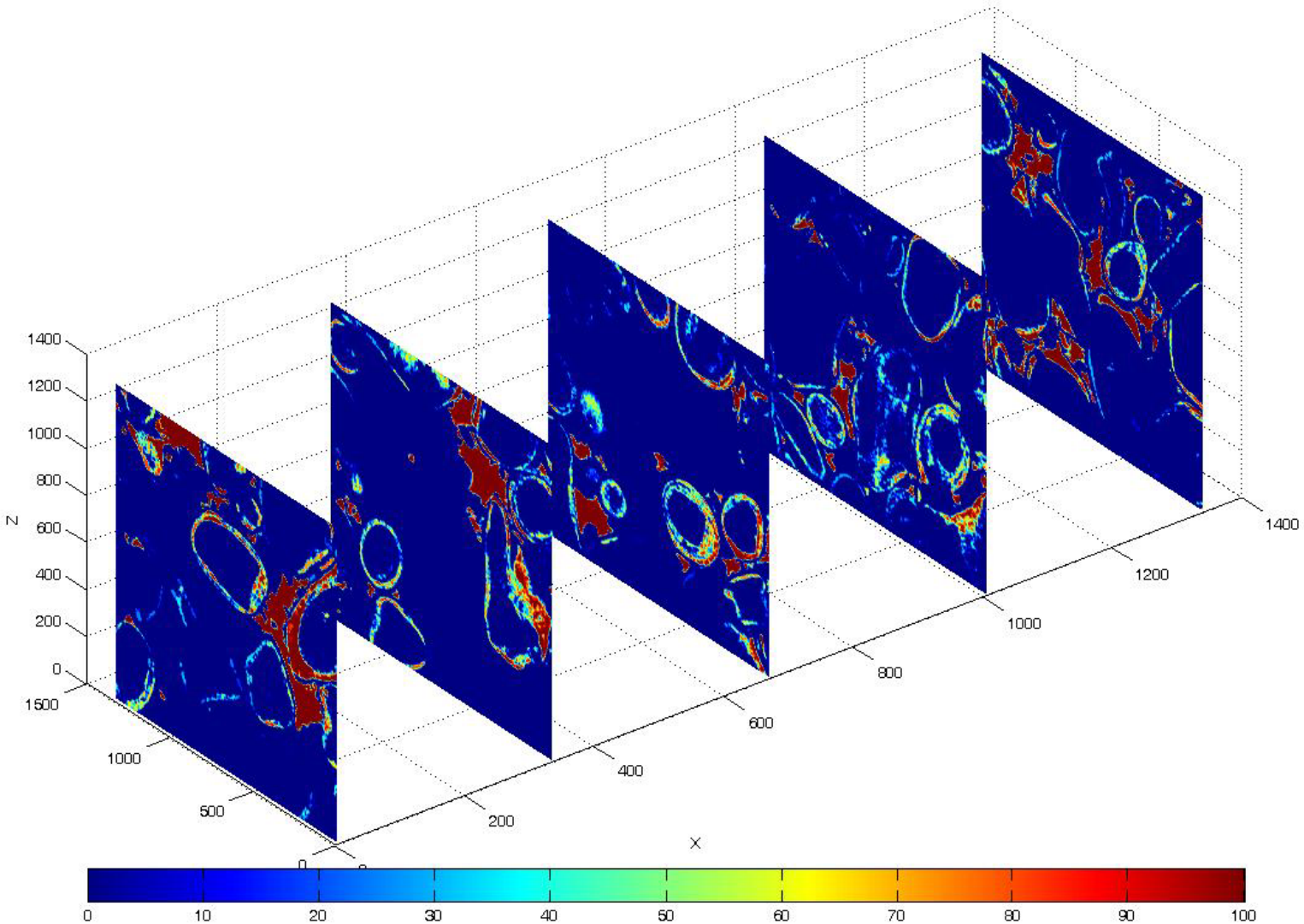

local porosity, %

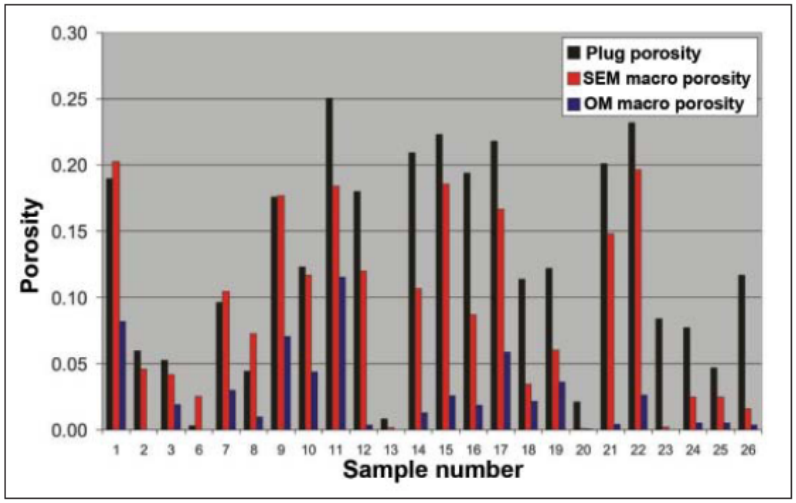

Figure 1. Total porosity compared to macroporosity measured on images acquired by optical light microscopy (OLM) and scatter electron microscopy (SEM) at similar pixel resolution.

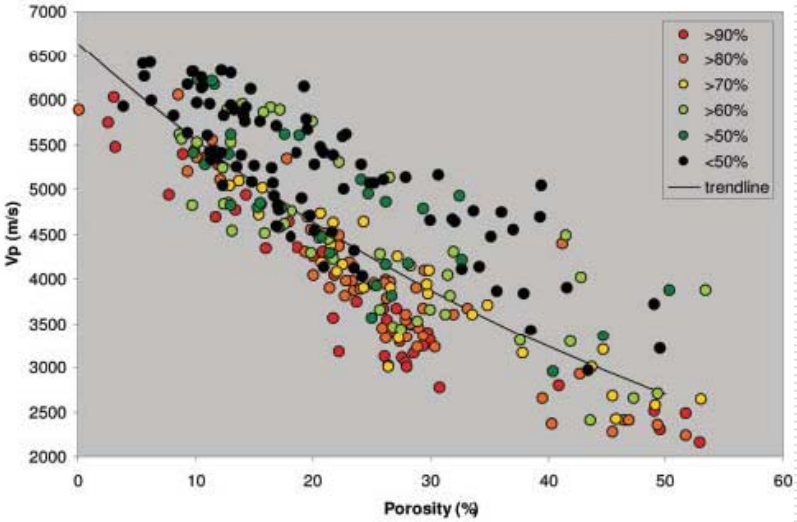

Plot of porosity versus P-wave velocity with color indicating the percentage of the total porosity due to micropores.

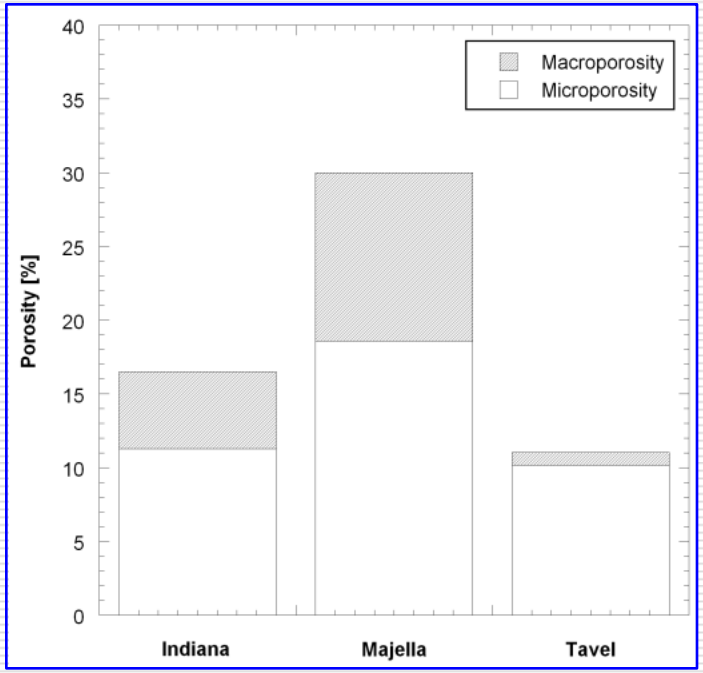

***Zhu, Baud & Wong* (2010)**

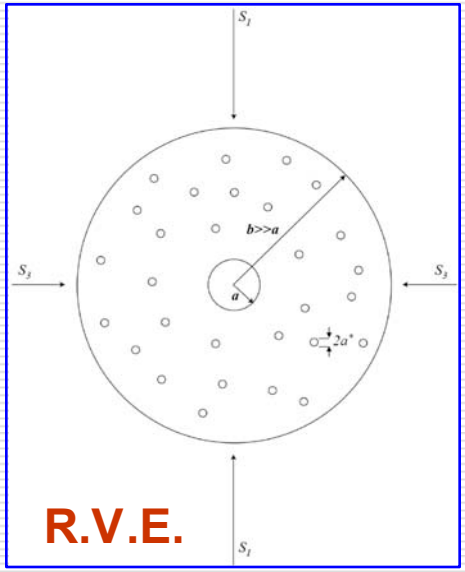

Effects of microporosity on sonic velocity in carbonate rocks

Gregor T. Baechle, ExxonMobil Upstream Research Company, Houston, USA
Arnout Colpaert, StatoilHydro Research Center, Trondheim, Norway
Gregor P. Eberli, University of Miami, USA
Ralf J. Weger, Repsol-YPF, Buenos Aires, Argentina

The Leading Edge August 2008

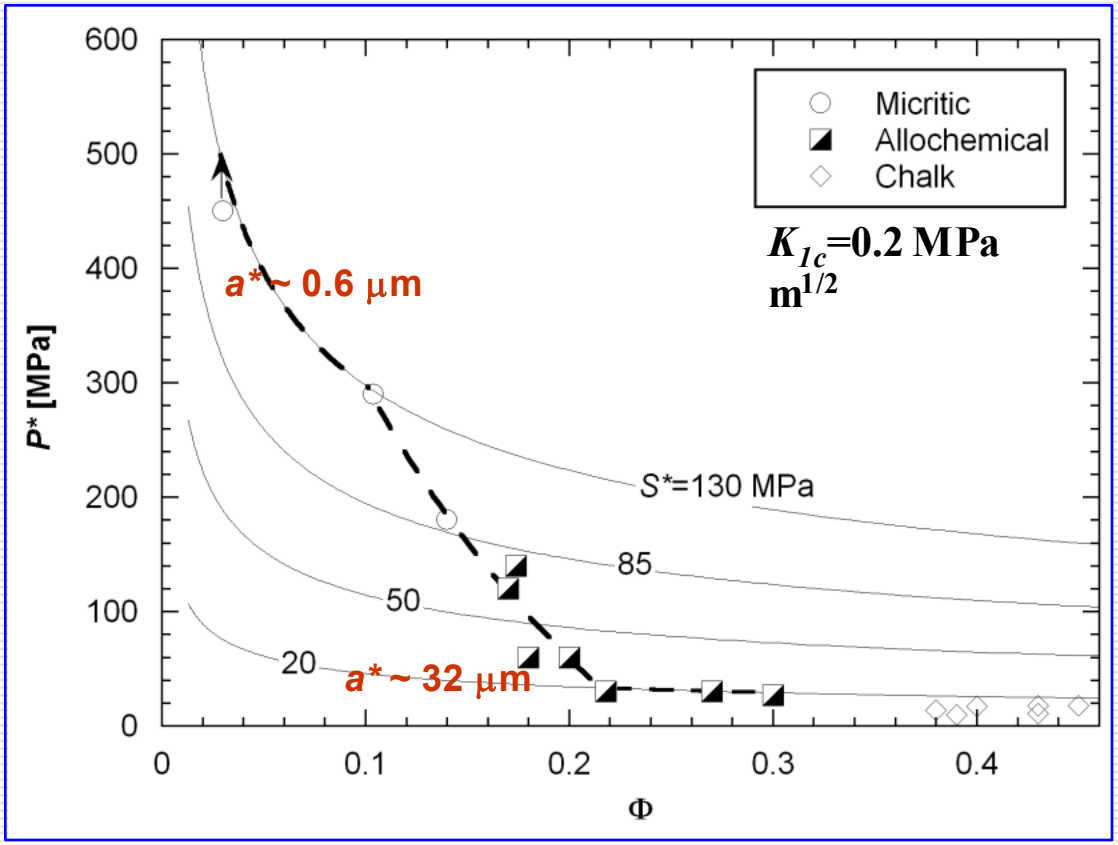

The critical pressure

- **decreases with increasing porosity following a power law**
- **scales with the inverse square root of mean micropore size**
- **is dependent on the partitioning between macro- and micro-porosity**

$$P^* = \frac{2}{3}\sigma_u^* = \frac{0.883}{\Phi_*^{0.414}} \frac{K_{IC}}{\sqrt{\pi a^*}} = \frac{0.883}{\Phi^{0.414}} S^*$$

Zhu, Baud & Wong (2010), *JGR*

$$S^* = \frac{K_{IC}}{(\Phi_* / \Phi)^{0.414} \sqrt{\pi a^*}}$$

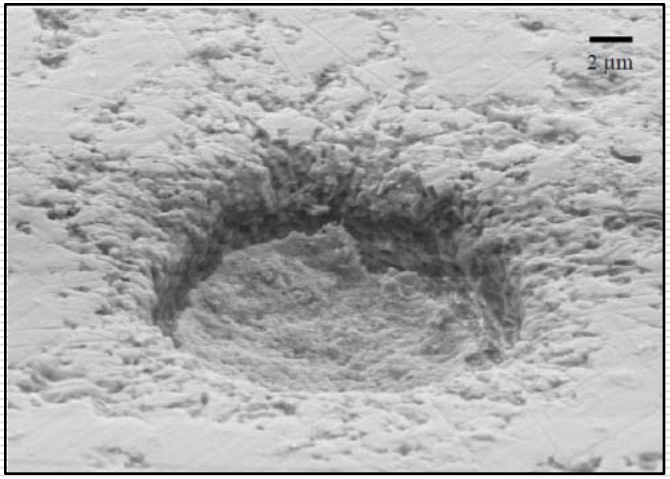

Inelastic Compaction in a Dual Porosity Medium

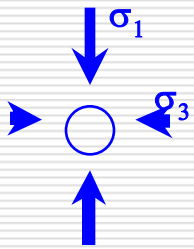

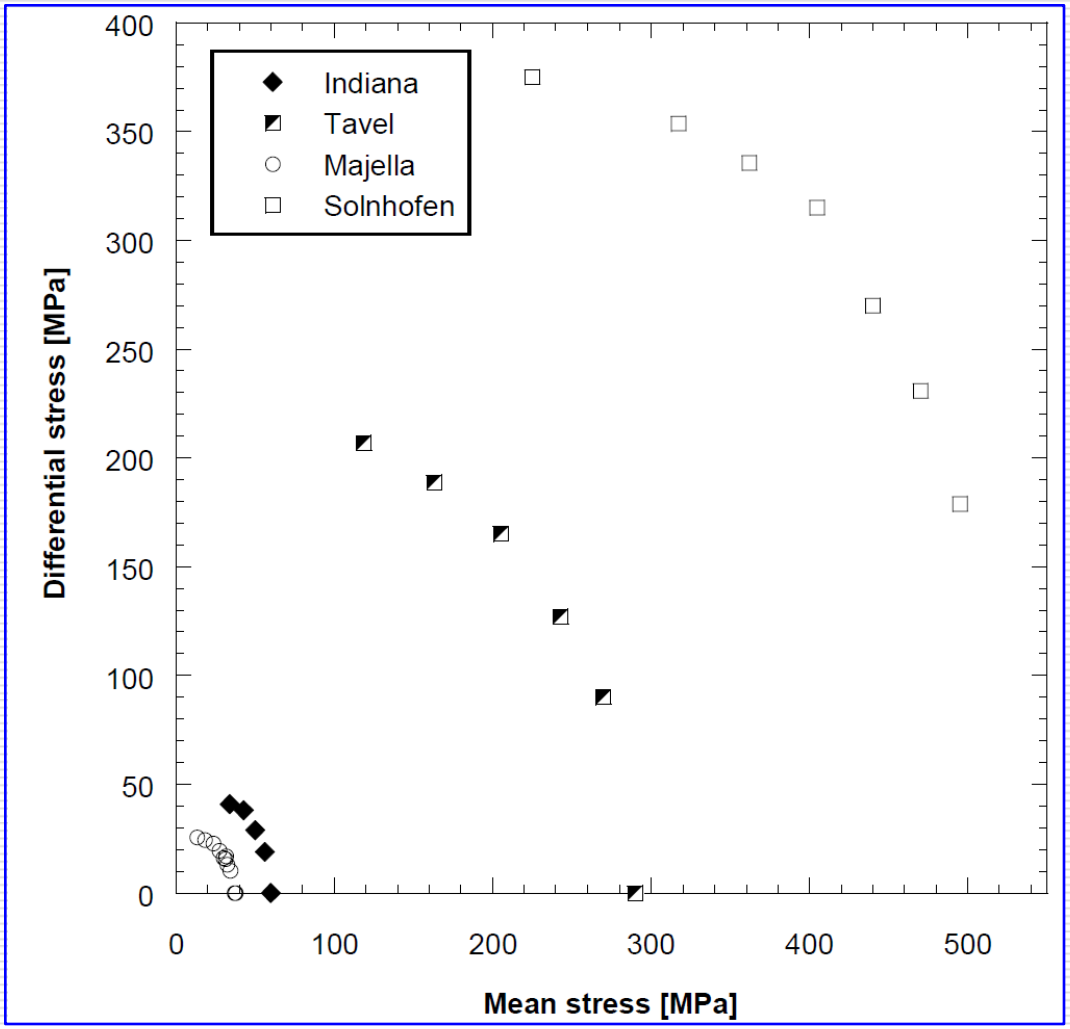

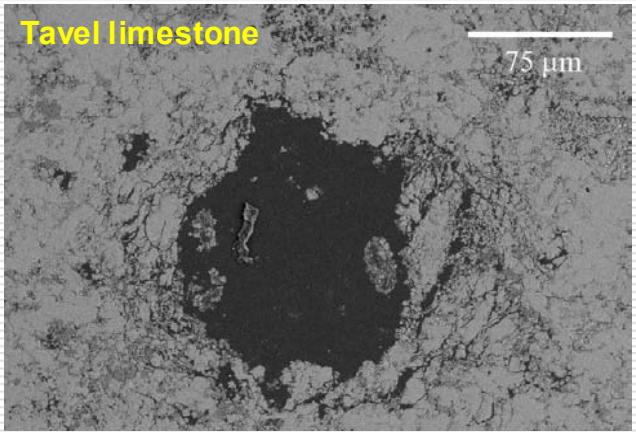

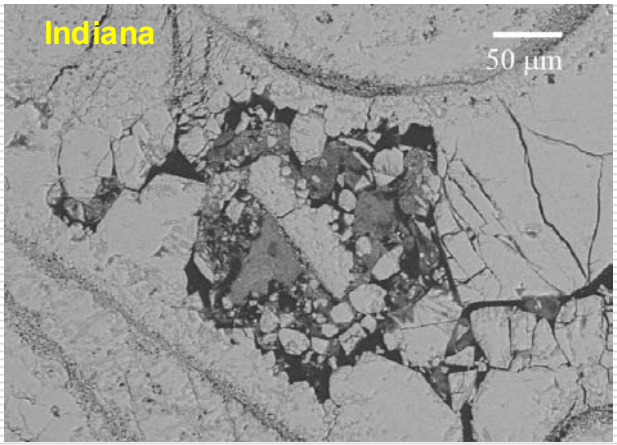

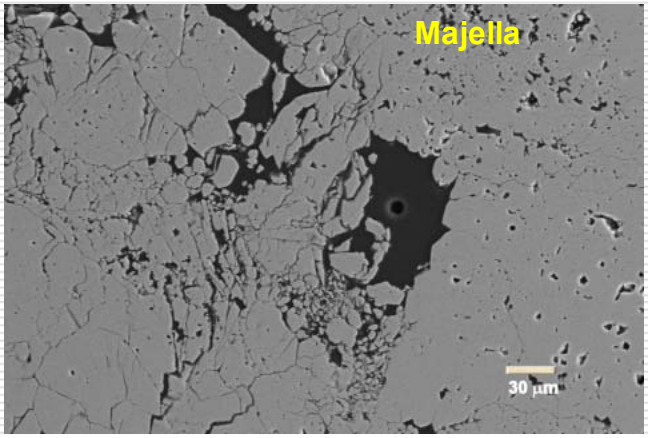

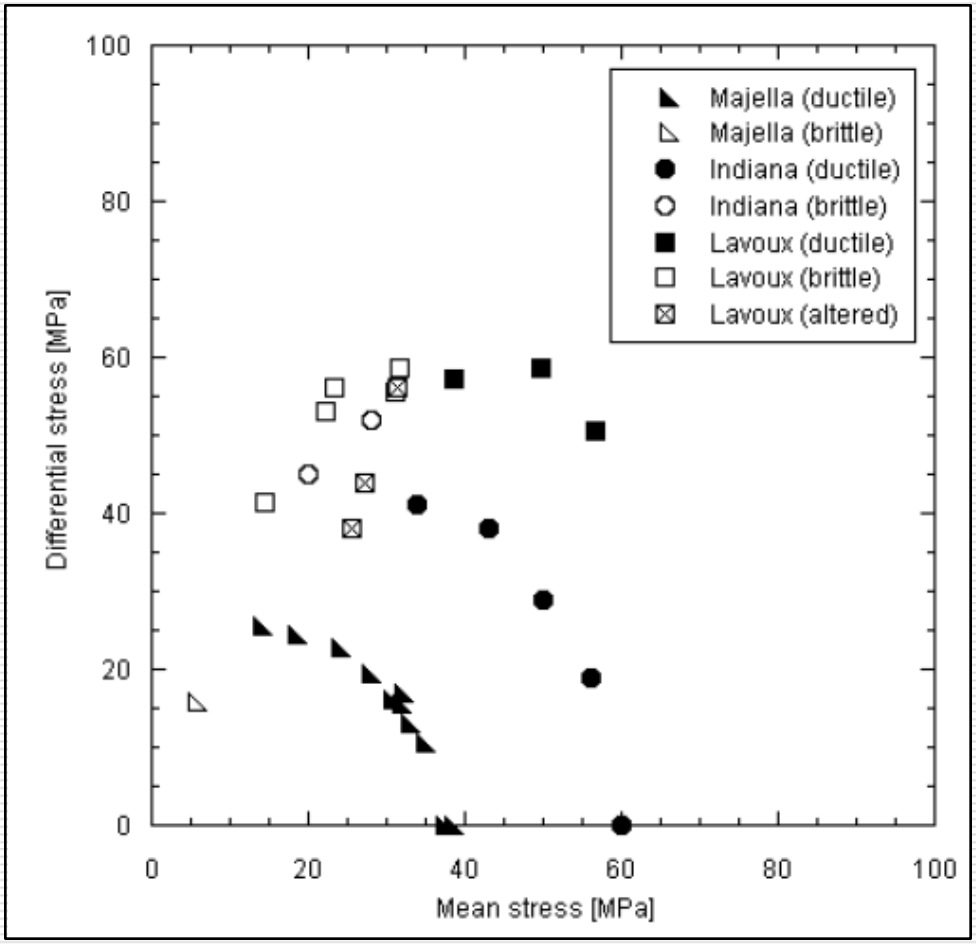

Figure 3. The brittle strength (open symbols) and compactive yield stress (solid symbols) of three limestones with porosities in the range of 20-30%. There is an overall trend for both brittle strength and yield stress to decrease with increasing porosity. Note that the chemically altered samples of Lavoux limestone first underwent dissolution by a "retarded acid", which resulted in relatively homogeneous porosity enhancement of up to 3% that was manifested by appreciable decrease in the brittle strength (at 12.7 MPa effective pressure). [After *Vajdova et al.*, 2004; *Zhu et al.*, 2009; *Bemer and Lombard*, 2009].

Picture of intact and altered Lavoux limestone samples (I = Intact sample, SAT = sample submitted to a Standard Acid Treatment, RAT = sample submitted to a Retarded Acid Treatment).

***Bemer & Lombard* (2009)**